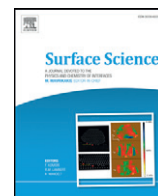




Contents lists available at ScienceDirect

Surface Science

journal homepage: [www.elsevier.com/locate/susc](http://www.elsevier.com/locate/susc)

## Contributions of dispersion forces to R-3-methylcyclohexanone physisorption on low and high Miller index Cu surfaces

Daniel S. Wei<sup>a</sup>, Bharat S. Mhatre<sup>b</sup>, Andrew J. Gellman<sup>b</sup>, David S. Sholl<sup>a,\*</sup>

<sup>a</sup> School of Chemical & Biomolecular Engineering, Georgia Institute of Technology, 311 Ferst Drive NW, Atlanta, GA 30332, USA

<sup>b</sup> Department of Chemical Engineering, Carnegie Mellon University, 5000 Forbes Avenue, Pittsburgh, PA 15213, USA

### ARTICLE INFO

Available online xxxx

#### Keywords:

Density functional theory

Physisorption

Temperature programmed desorption

### ABSTRACT

The physisorption of R-3-methylcyclohexanone on low and high Miller index Cu surfaces is studied with temperature programmed desorption (TPD) and density functional theory (DFT). The DFT calculations are performed with D2, vdW-optB86b, and vdW-optB88 dispersion corrected methods. The adsorption energies calculated by the dispersion corrected methods are more comparable to the TPD results than those calculated without dispersion corrections, although, the former methods have a tendency to overbind the surface adsorbates. The implementation of dispersion corrected methods also indicates a possible adsorbate induced surface reconstruction on Cu(110).

© 2014 Elsevier B.V. All rights reserved.

### 1. Introduction

Kohn–Sham Density functional theory (KS-DFT) is an important tool in the study of surface–adsorbate interactions [1,2]. Using the local density approximation (LDA) or the generalized gradient approximation (GGA) functional, DFT is able to predict adequately the behavior of atoms or small chemisorbed species on metal surfaces. However, as adsorbate size increases, weak dispersion forces become significant for many physisorbed species. Neither LDA nor GGA can correctly describe these dispersion forces [3,4]. Grimme sought to address these drawbacks with the introduction of a semi-empirical dispersion force correction to the GGA functional [5,6]. Soler and others also tried to account for the dispersion forces by using non-local van der Waals density functionals [7,8]. The optimized B86b method uses a new gradient-corrected exchange energy to account for interaction in systems with large density gradient [9,10]. The optimized B88 method further improves this through a proper asymptotic potential for the gradient-corrected exchange energy approximation [4,11,12]. These dispersion corrected methods have been shown to significantly increase the adsorption energies calculated using DFT and improve agreement with experimental data [13–17]. Peköz et al. reported that the adsorption energy of dichlorobenzene on Au and Pt surfaces increased from the negligible value of 0.1 eV to 1.0–1.1 eV after correcting the conventional GGA with the vdW-DFT method [18]. A study of benzene, thiophene, and pyridine adsorption on Au(111) and Cu(111) by Tonigold and Gross achieved better agreement with experimental data using DFT-D than when

using the nonhybrid GGA, although, their calculations also revealed a tendency of DFT-D to overbind adsorbates to metal substrates [19].

The emergence of dispersion force corrections to DFT methods has allowed us to reexamine interesting adsorbates for which physisorption forces are expected to contribute significantly to adsorption. One such interaction is the enantioselective adsorption of chiral hydrocarbons on naturally chiral surfaces [20–24]. Temperature-programmed desorption (TPD) has revealed measurable enantiospecific differences in the desorption energies of enantiomers such as 3-methylcyclohexanone and propylene oxide from chiral Cu surfaces [25–29]. Those studies examined intrinsically chiral Cu single crystal surfaces created by cleaving normal to a low symmetry direction of the achiral FCC crystal [30–32]. The adsorption and desorption of R-3-methylcyclohexanone (R-3MCHO) have been studied on a large set of Cu single crystal surfaces that spans the stereographic triangle and includes the three low Miller index surfaces Cu(111), Cu(110) and Cu(100), six stepped surfaces Cu(221), Cu(771), Cu(533), Cu(511), Cu(410) and Cu(430), and seven kinked surfaces Cu(643)<sup>R&S</sup>, Cu(653)<sup>R&S</sup>, Cu(17,5,1)<sup>R&S</sup>, Cu(13,9,1)<sup>R&S</sup>, Cu(821)<sup>R&S</sup>, Cu(651)<sup>R&S</sup>, and Cu(531)<sup>R&S</sup>. Cu(*hkl*) surfaces that have  $h \neq k \neq l$  and  $h \cdot k \cdot l \neq 0$  are intrinsically chiral and exist in two enantiomorphous forms denoted as (*hkl*)<sup>R</sup> and (*hkl*)<sup>S</sup>. TPD results show that the desorption energies,  $\Delta E_{\text{des}}$ , of R-3MCHO from the terraces are roughly equivalent on all surfaces, as are the desorption energies from the step sites and the kink sites. Not surprisingly, the trend among the desorption energies is  $\Delta E_{\text{des}}^{\text{terr}} < \Delta E_{\text{des}}^{\text{step}} < \Delta E_{\text{des}}^{\text{kink}}$ . However, on the enantiomorphs of the chiral surfaces there are measurable enantiospecific differences of ~1 kJ/mol in the desorption energies from the enantiomorphous kinks:  $\Delta E_{\text{des}}^{\text{R-kink}} \neq \Delta E_{\text{des}}^{\text{S-kink}}$ . Using the PW-91 functional, DFT simulation of the adsorption energy of R-3MCHO from Cu(111) and Cu(322) yielded values that were ~0.45 eV

\* Corresponding author.

E-mail addresses: [daniel.wei@chbe.gatech.edu](mailto:daniel.wei@chbe.gatech.edu) (D.S. Wei), [bmhatre@andrew.cmu.edu](mailto:bmhatre@andrew.cmu.edu) (B.S. Mhatre), [gellman@cmu.edu](mailto:gellman@cmu.edu) (A.J. Gellman), [david.sholl@chbe.gatech.edu](mailto:david.sholl@chbe.gatech.edu) (D.S. Sholl).

lower than the experimental values [33]. This discrepancy was attributed to PW91's inability to account for dispersion contributions to the binding of R-3MCHO to the Cu surfaces. A similar study using the non-hybrid PBE functional estimated the benzene desorption energy on Cu(111) to be  $-0.06$  eV [34], but experiments estimate the adsorption energy between  $-0.53$  and  $-0.62$  eV [35,36]. Here we use R-3MCHO adsorption on Cu surfaces as a benchmark test for several dispersion corrected DFT methods. This study utilizes DFT and TPD to quantify the effectiveness of various dispersion force corrected methods for predicting surface-adsorbate interaction by examining R-3MCHO physisorption behavior on the low and high Miller index Cu surfaces.

## 2. Methods

### 2.1. Density functional theory

Periodic DFT calculations were conducted with the Vienna *Ab initio* Simulation Package (VASP) [37–40]. The electron–electron exchange and correlation interactions were described with the PBE–GGA functional [41,42]. Core–electron interactions were modeled with the projector augmented-wave (PAW) potential [43,44]. All calculations used a plane wave expansion cutoff of 500 eV. Structural optimization was performed by a conjugate gradient algorithm with a force stopping criterion of 0.03 eV/Å. The study utilized Grimme's D2 (PBE–D2), the vdW\_optB86b (PBE–B86b), and the vdW\_optB88 (PBE–B88) dispersion corrected methods [6,12]. Bulk Cu atoms were examined with 8 Cu atoms in an FCC lattice using  $16 \times 16 \times 16$  k-points. The atomic positions, unit cell shape, and unit cell size were allowed to relax for each dispersion corrected method. The lattice constants are reported in Table 1. The Cu lattice constants predicted by PBE–D2, PBE–B86b, and PBE–B88 were found to be 1.74%, 0.85%, and 0.10% smaller, respectively, than the lattice constant calculated by PBE–GGA. All surface calculations were performed using the optimized lattice constant determined using the functional used in that calculation.

All surface calculations had a vacuum spacing of at least 10 Å. The required slab thickness was determined with R-3MCHO adsorption on Cu(111). The minimum thickness was achieved when the presence of an additional layer changed the R-3MCHO adsorption energy by less than 0.05 eV. This was determined to be three Cu(111) layers with the bottommost layer immobilized. Unless otherwise stated, surfaces were modeled as an approximately 7 Å thick slab with the bottommost 3 Å immobilized. Molecules were only adsorbed on one side of the slab. The low Miller index Cu(111), Cu(100), and Cu(110) surfaces were made up of  $p(5 \times 5)$  surface unit cells and were examined with  $3 \times 3 \times 1$  k-points. The stepped Cu(221) and Cu(322) surfaces were modeled with  $p(2 \times 6)$  surface unit cells. The kinked Cu(643)<sup>R</sup> consisted of only one surface unit cell. Calculations for the latter three surfaces used  $2 \times 2 \times 1$  k-points. The resolution in k-points were chosen to ensure good convergence while reducing computational cost. Table 2 below demonstrated that these k-points offer sufficient convergence for our study.

Calculations were also performed for a reconstructed Cu(110) surface to mimic the  $(2 \times 1)$  missing-row reconstruction seen for Pt(110) [45–47]. The  $(2 \times 1)$  reconstructed Cu(110) surface was modeled with a slab approximately 10 Å thick with the bottommost 5 Å immobilized. The reconstructed Cu(110) supercell had a  $p(2 \times 5)$  surface unit cell

**Table 1**  
Bulk Cu lattice for each dispersion corrected method.

| Functional | Lattice |
|------------|---------|
| PBE–GGA    | 3.63    |
| PBE–D2     | 3.57    |
| PBE–B86b   | 3.60    |
| PBE–B88    | 3.63    |

**Table 2**

The total adsorption energy of R-3MCHO per unit cell on different surfaces as a functional of resolution in k-points.

|                       | Cu(111) | Cu(100) | Cu(110) | Cu(221) | Cu(643) <sup>R</sup> |
|-----------------------|---------|---------|---------|---------|----------------------|
| $1 \times 1 \times 1$ | −1.16   | −1.20   | −1.22   | −1.40   | −1.58                |
| $2 \times 2 \times 1$ | −1.02   | −1.18   | −1.14   | −1.50   | −1.49                |
| $3 \times 3 \times 1$ | −1.05   | −1.17   | −1.17   | −1.44   | −1.51                |
| $4 \times 4 \times 1$ | −1.04   | −1.18   | −1.15   | −1.46   | −1.52                |

and used  $2 \times 2 \times 1$  k-points. A single R-3MCHO was placed on each computational supercell to simulate adsorption. The isolated R-3MCHO molecule in a  $20 \times 20 \times 20$  Å cell was sampled only at the  $\Gamma$  point. Various geometric configurations were examined, and the lowest energy state was used as the reference state. On the clean surface, the adsorption energy was defined as,

$$\Delta E_{\text{Adsorption}} = E_{\text{total}} - E_{\text{3MCHO}} - E_{\text{Surface}} \quad (1)$$

where  $E_{\text{total}}$ ,  $E_{\text{3MCHO}}$ ,  $E_{\text{Surface}}$  are the total energy of the relaxed structure including the adsorbed molecule, the energy of the isolated R-3MCHO, and the clean surface energy, respectively. For the reconstructed surface, the adsorption energy had to account for the energy lost to the reconstruction. The effective adsorption energy was defined as,

$$\Delta E_{\text{Effective adsorption}} = E_{\text{total}} - E_{\text{3MCHO}} - E_{\text{Reconstructed surface}} - A^* \Delta E_{\text{Reconstruction}} \quad (2)$$

where  $E_{\text{Reconstructed surface}}$  is the total energy of the clean reconstructed surface,  $A$  is the reconstructed surface area, and  $\Delta E_{\text{Reconstruction}}$  is the energy required to reconstruct  $1 \text{ \AA}^2$  of the surface. A negative  $\Delta E_{\text{Reconstruction}}$  denoted an unfavorable reconstruction as the surface required energy from the environment to undergo reconstruction.

Multiple preferred adsorption configurations and location combinations were systematically examined for each surface. A list of possible adsorption geometries for each surface was generated by placing oxygen on a large number of possible high symmetry surface sites and allowing the methylcyclohexane group to rotate around the oxygen. On high Miller index surface, special attention was paid to examine geometries where the methylcyclohexane group was on top of the stepped or kinked sites. Typically, these initial geometries converged to a few selective local minima, and only the most energetically preferred states were used in this study.

### 2.2. TPD experimental methods

TPD has been used to measure the influence of surface structure on the desorption energies of R-3MCHO from a large set of Cu(*hkl*) single crystal surfaces and under ultra-high vacuum (UHV) conditions. Details of the experimental measurements can be found in prior publications [26,28,48,49]. Briefly, the single crystal surfaces were cleaned in UHV by cycles of Ar<sup>+</sup> ion sputtering and annealing at temperatures in the range 800–1000 K. The orientation and the crystallinity of the surfaces were examined using low energy electron diffraction. Once the Cu surfaces were clean, R-3MCHO was adsorbed at temperatures of  $\sim 170$  K by exposure of the surfaces to vapor introduced into the UHV chamber through a leak valve. The adsorption temperature of 170 K limited the coverage to one monolayer and prevented the formation of condensed multilayers. TPD of the adsorbed monolayer was performed by positioning the Cu single crystal in front of the aperture to a mass spectrometer and heating the crystal at 1 K/s while monitoring the signal at  $m/q = 39$  amu.

Download English Version:

<https://daneshyari.com/en/article/5422127>

Download Persian Version:

<https://daneshyari.com/article/5422127>

[Daneshyari.com](https://daneshyari.com)